Tissue of origin dictates branched-chain amino acid metabolism in mutant Kras-driven cancers

HHS Public Access

Author manuscript

Science. Author manuscript; available in PMC 2017 January 19.

Published in final edited form as:

Science. 2016 September 09; 353(6304): 1161–1165. doi:10.1126/science.aaf5171.

Tissue-of-origin Dictates Branched-Chain Amino Acid Metabolism in Mutant *Kras*-driven Cancers

Jared R. Mayers[1,2,*], **Margaret E. Torrence**[1,2,*], **Laura V. Danai**[1], **Thales Papagiannakopoulos**[1,†], **Shawn M. Davidson**[1,2], **Matthew R. Bauer**[1], **Allison N. Lau**[1], **Brian W. Ji**[3], **Purushottam D. Dixit**[3], **Aaron M. Hosios**[1,2], **Alexander Muir**[1], **Christopher R. Chin**[1], **Elizaveta Freinkman**[1,2,4,5,6], **Tyler Jacks**[1,2,6], **Brian M. Wolpin**[7], **Dennis Vitkup**[3], and **Matthew G. Vander Heiden**[1,2,5,7,‡]

[1]Koch Institute for Integrative Cancer Research, Massachusetts Institute of Technology, Cambridge, Massachusetts 02139, USA

[2]Department of Biology, Massachusetts Institute of Technology, Cambridge, Massachusetts 02139, USA

[3]Center for Computational Biology and Bioinformatics and Initiative in Systems Biology, Columbia University, New York, New York 10027, USA

[4]Whitehead Institute for Biomedical Research, Nine Cambridge Center, Cambridge, Massachusetts 02142, USA

[5]Broad Institute, Seven Cambridge Center, Cambridge, Massachusetts 02142, USA

[6]Howard Hughes Medical Institute, Massachusetts Institute of Technology, Cambridge, Massachusetts 02139, USA

[7]Dana-Farber Cancer Institute, Boston, Massachusetts 02115, USA

Abstract

Tumor genetics guides patient selection for many new therapies, and cell culture studies have demonstrated that specific mutations can promote metabolic phenotypes. However, whether tissue context defines cancer dependence on specific metabolic pathways is unknown. *Kras* activation and *Trp53* deletion in the pancreas or the lung result in pancreatic ductal adenocarinoma (PDAC) or non-small cell lung carcinoma (NSCLC) respectively, but despite the same initiating events, these tumors utilize branched-chain amino acids (BCAAs) differently. NSCLC tumors incorporate free BCAAs into tissue protein and use BCAAs as a nitrogen source while PDAC tumors have decreased BCAA uptake. These differences are reflected in expression levels of BCAA catabolic enzymes in both mice and humans. Loss of Bcat1 and Bcat2, the enzymes responsible for BCAA

[‡]Correspondence: Matthew G. Vander Heiden, +1–617–715–4471, mvh@mit.edu.
[*]Equal contribution
[†]Current Address: School of Medicine, New York University, New York, New York 10016, USA

Supplementary Materials:
Materials and Methods
Figures S1–S10
Tables S1–S8
References (40–49)

utilization, impairs NSCLC tumor formation, but these enzymes are not required for PDAC tumor formation, arguing that tissue-of-origin is an important determinant of how cancers satisfy their metabolic requirements.

Main Text

The development of new cancer therapeutics relies on underlying genetic features to identify sensitive patients (1). Mutations in both *KRAS* and *TP53* are common genetic events found in tumors arising from many tissues and cancers with these mutations are often difficult to treat (2, 3). These genetic events, as well as others associated with cancer, contribute to the metabolic changes that support biomass accumulation and cancer cell proliferation (4). Oncogenic RAS signaling increases glucose and glutamine consumption to support anabolic processes including nucleotide, lipid and non-essential amino acid biosynthesis and can also drive extracellular protein and lipid scavenging (5). *TP53* mutations increase glucose consumption and glycolytic flux, while inactivation of *TP53* renders cancer cells more dependent on serine uptake and metabolism (6).

KRAS and *TP53* mutations are found in most human pancreatic tumors (7) and are also common in lung adenocarcinoma (8). How mutant *KRAS* or disruption of *TP53* affect cancer metabolism is based on cell culture studies in defined medium, although *in vivo* nutrient availability varies widely between tissues and vasculature changes can limit nutrient access within tumors (9, 10). The inability to model these differences in culture has therefore limited understanding of how tissue-of-origin influences tumor metabolism (11). Furthermore, environment can influence metabolic phenotypes *in vitro* (12–14), and metabolic dependencies *in vivo* can differ from those found *in vitro* (15). Metabolic differences between tumor types may also result from cell-autonomous effects, and tumor metabolic gene expression more closely resembles that of its tissue-of-origin than that of other tumors (16). The same oncogenic driver can also cause different metabolic phenotypes in lung and liver tumors (17). This raises the possibility that tumor type is a major determinant of some tumor metabolic dependencies *in vivo*.

Elevated plasma BCAA levels are found in early PDAC, but not in NSCLC, even when the tumors are initiated by the same genetic events (18). To confirm that tumor tissue-of-origin influences whole-body BCAA metabolism, we utilized *LSL–Kras*$^{G12D/+}$*; Trp53*$^{flox/flox}$ (KP) mice. We crossed KP mice to mice harboring a *Cre-recombinase* allele driven by a *Pdx-1* promoter (KP$^{-/-}$C model) (19) or delivered viral *Cre* to the lungs of these mice (20) to generate models of PDAC and NSCLC respectively. Consistent with prior reports (18), mice with early PDAC have increased levels of plasma BCAAs while mice with early NSCLC exhibit decreased plasma BCAA levels (figs. S1, A–D). When cells derived from these tumors are implanted subcutaneously into syngeneic hosts, tumors derived from PDAC cells did not affect plasma BCAA levels (fig. S1E) (18), while tumors derived from NSCLC cells led to decreased plasma BCAAs (fig. S1F). These results suggest that tumor formation from NSCLC cells can cause depletion of circulating BCAAs.

To trace tissue-specific differences in BCAA metabolism in animals with pancreatic or lung tumors, mice were fed an amino acid defined diet in which 20% of leucine and valine

were ^{13}C-labeled. All groups of mice exhibited similar levels of plasma ^{13}C-BCAA enrichment after one-week exposure to labeled diets (figs. S2, A and B). While PDAC tumors contained slightly decreased free BCAAs relative to normal pancreas, NSCLC tumors displayed a significant increase in labeled free BCAAs compared to normal lung (Fig. 1A and figs. S2, C and D). Importantly, these differences are not a reflection of different amino acid compositions of normal or tumor tissue in either the PDAC or NSCLC models (fig. S3). Because BCAAs are essential amino acids that animals cannot synthesize *de novo* (21), these results suggest that unlike PDAC tumors, NSCLC tumors display enhanced BCAA uptake.

BCAAs have several potential metabolic fates in tissues (Fig. 1B). They can be directly incorporated into protein or reversibly transaminated by branched-chain amino acid transaminase (Bcat) to produce branched-chain α-ketoacids (BCKAs) and glutamate. BCKAs can regenerate BCAAs, be secreted, or be oxidatively decarboxylated by the branched-chain keto-acid dehydrogenase (Bckdh) complex to allow further oxidation of the carbon skeleton (21). In agreement with increased BCAA uptake in NSCLC tumors, lung tumors displayed increased labeled BCAA incorporation into protein compared to normal lung, while PDAC tumors incorporated less labeled BCAAs relative to normal pancreas (Fig. 1C and figs. S2, E and F). Analysis of metabolites derived from BCAA catabolism revealed that NSCLC tumors also had more labeled α-ketoisocaproate (KIC), the leucine-derived BCKA, while no change was observed in levels of this labeled metabolite in PDAC tumors (Fig. 1D and fig. S2G). No other differences in labeled BCAA catabolite levels were observed in NSCLC compared to normal tissues, but PDAC tumors showed decreased labeling of the tricarboxylic acid (TCA) cycle intermediate citrate relative to normal pancreas from labeled BCAAs (Fig. 1E and figs. S2, G–I). This is consistent with recent work demonstrating minimal catabolism of BCAAs to TCA intermediates in proliferating cells (22). We then explored whether excess KIC may be excreted by NSCLC tumors for further metabolism by other tissues such as liver, which has limited Bcat, but high Bckdh activity (21, 23). Consistent with this hypothesis, we observe increased labeling of downstream leucine metabolites in the livers of mice with lung tumors (fig. S4). Taken together, these data suggest that BCAA uptake and transamination, but not their subsequent catabolism, may provide a benefit to NSCLC tumors, potentially by acting as a source of nitrogen.

To examine whether NSCLC tumors, but not PDAC tumors, use BCAAs as a source of nitrogen, we fed mice a modified amino acid diet where 50% of leucine was labeled with ^{15}N, allowing the fate of leucine-derived nitrogen to be traced (Fig. 2A). In agreement with ^{13}C-tracing, mice with PDAC demonstrated no differences in free ^{15}N-labeled leucine in tumors compared to control pancreas (fig. S5A), and had less ^{15}N incorporation into other amino acids (fig. S5B). In contrast, increased levels of ^{15}N-leucine were found in NSCLC tumors compared to normal lung (fig. S5C) with decreased plasma enrichment of ^{15}N-leucine in mice with NSCLC tumors (Fig. 2B and fig. S5D). A relative increase in ^{15}N-labeling of non-essential amino acids, as well as valine and isoleucine, was observed in both the free and tissue-protein amino acid pools of NSCLC compared to control lung (Fig. 2C and figs. S5, C and E). Given the reduced plasma enrichment transamination mediated by *Bcat* isoforms is active in NSCLC tumor tissue. Evidence for increased BCAA

transamination in NSCLC compared to PDAC cells is also evident *in vitro* across a range of glutamine concentrations, however tissue culture does not recapitulate the same phenotypes observed in tumors (fig. S6). Downstream of non-essential amino acid biosynthesis, this nitrogen can also be used to generate nucleotides, primarily if aspartate is synthesized *de novo* in these tumors. Consistent with this possibility, we find increased incorporation of ^{15}N-label in both aspartate and nucleotides (Figs. 2, C and D and fig. S5E). In some contexts, aspartate production is limiting for nucleotide biosynthesis and proliferation (24, 25), indicating that BCAA metabolism may be important for tumor growth.

To test whether gene expression differences might contribute to differential BCAA metabolism, we used quantitative RT-PCR to analyze mRNA levels in NSCLC and PDAC tumors compared to their respective normal tissues. Consistent with increased BCAA uptake and KIC generation in NSCLC tumors, these tumors displayed increased expression of the primary BCAA transporter *Slc7a5* (also called the neutral amino acid transporter *Lat1*) and increased levels of *Bcat2* and *Bckdh* (Figs. 3, A, C and D). In contrast, PDAC exhibited decreased expression of these genes relative to normal pancreas (Figs. 3, B–D). Importantly, we also observed increased inhibitory phosphorylation of the Bckdh complex in lung tumors (Figs. 3, C and D). *Bcat* expression enables utilization of BCAAs as a source of nitrogen by lung tumors, and inhibition of Bckdh prevents further catabolism of these amino acids.

The expression changes observed in PDAC are not unique to this model, as the related KPC mouse model (26), which is initiated by a point mutation in *Trp53*, showed similar changes in gene expression (fig. S7A). Furthermore, these decreases in gene expression do not appear to be a consequence of the relative decrease in cancer cellularity of PDAC tumors (7), as sorted pancreatic cancer cells showed similar expression of genes involved in proximal BCAA catabolism relative to whole tumor extracts (fig. S7B). In further agreement with neither lung nor pancreatic cancers showing evidence of downstream BCAA-carbon oxidation, the expression of enzymes from this pathway was not markedly different in either of these cancers (figs. S7, C and D). In contrast, glycolytic gene expression was increased in both tumor types (figs. S7, E and F), which is consistent with known increases in glycolysis in each tumor type (27–29). Finally, to relate these data to tissue-of-origin, we performed principal component and clustering analyses, which demonstrated segregation of each tumor with the normal tissue from which it arose (figs. S7, G and H).

To ascertain whether similar changes in gene expression were also found in human cancers, we examined expression of BCAA catabolic enzymes in NSCLC and PDAC relative to their respective normal tissues in publically available data sets (30). Consistent with our observations in mice, human NSCLC had increased expression of *SLC7A5*, *BCAT*, and *BCKDH*, while expression of BCAA catabolism pathway enzymes was decreased in human PDAC ($P < 0.0001$ for the pathway) (Fig. 3E and tables S1 and S2). The distinct expression patterns for each tumor type were highly correlated across multiple data sets (fig. S7I and tables S3–6). Interestingly, the similarity between human NSCLC and the mouse model of NSCLC was observed despite *KRAS* and *TP53* mutations occurring in less than 50% of human tumors (8) and similar expression patterns were also seen in squamous cell lung cancer (fig. S7I and table S6), further supporting the notion that tissue-of-origin can dictate metabolic phenotype.

The increased contribution of plasma BCAAs to biomass in NSCLC tumors suggests that these tumors may rely on BCAA metabolism for growth. To test this possibility, we used CRISPR-Cas9 mediated genome editing to disrupt exon sequences present in both the *Bcat1* (cytosolic) and the *Bcat2* (mitochondrial) isoforms (fig. S8A) in cancer cell lines derived from KP mice with NSCLC (*Bcat* null Clones A and B) or PDAC (*Bcat* null) (fig. S8B). Expression analysis and ^{15}N-leucine tracing studies confirmed functional deletion of *Bcat* in both the NSCLC and PDAC cancer cells (figs. S8, C–F). Despite loss of both *Bcat* isoforms, these cells proliferate at a rate that is similar to the parental and vector control infected cell lines *in vitro* (Figs. 4, A and B). When *Bcat* null NSCLC cells were implanted subcutaneously *in vivo*, however, the ability of these cells to form tumors was significantly impaired, and one clone failed to produce tumors (Fig. 4C and fig. S8G). In contrast, *Bcat* null PDAC cells implanted subcutaneously generated tumors (Fig. 4D and fig. S8H). Additionally, orthotopic transplantation of NSCLC *Bcat* null cells failed to form lung tumors (Fig. 4E), while PDAC *Bcat* null cells formed tumors in the pancreas (Fig. 4F). Unlike subcutaneously implanted PDAC *Bcat* knockout cells, these cells formed smaller tumors in the pancreas than control cells (fig. S8I). Taken together, these data suggest that while KP lung tumors require Bcat activity for growth, this enzyme activity is dispensable for KP pancreas tumor formation, although PDAC tumor growth may be aided by Bcat activity in some tissue environments.

Proliferating cells need to acquire amino acids, both to make protein and as source of nitrogen for nucleotide and non-essential amino acid synthesis. Prior work has shown that macropinocytosis plays a role in filling this requirement in mutant *RAS*-driven PDAC tumors and cells (12, 14, 31). The data presented here argue that this process might be less active in mutant *Ras* transformed NSCLC tumors that acquire nitrogen in part from free BCAAs. Indeed, we observed less macropinocytosis in cells derived from mouse NSCLC relative to mouse PDAC cells (fig. S9). The decreased reliance of PDAC on free BCAAs however, does not necessarily imply that uptake of these amino acids would be toxic for this cancer. Overexpressing *Slc7a5* in PDAC cells is sufficient to increase leucine uptake (figs. S10, A and B), but has minimal effects on proliferation *in vitro* (fig. S10C) or tumor growth *in vivo* (figs. S10, D and E).

A role for free BCAAs in supplying nitrogen to lung cancers is intriguing in light of recent studies in glioblastoma and NSCLC indicating that glutamine, which is the most abundant plasma amino acid and serves as the major free amino acid substrate for nitrogen and carbon in culture (32), contributes less to tumor metabolism *in vivo* (33, 34). Indeed, glucose-tracing studies in humans and mice demonstrate that glutamine is net synthesized from glucose (15, 33–37), and alternative sources of nitrogen are required to support glutamine production. Thus, in these contexts, extraction of nitrogen from BCAAs for *de novo* amino acid and nucleotide biosynthesis *in vivo* may explain how lung tumors satisfy their nitrogen requirements. Consistent with this possibility, *BCAT1* expression is known to be important for glioblastoma growth (38), suggesting that tumors arising in tissues other than the lung may also utilize BCAAs as a source of nitrogen. Multiple factors including local environment, tumor cell-of-origin, and genetic mutations can lead to convergent metabolic adaptations in disparate tumor types.

Elevations in plasma BCAA levels are associated with early PDAC and result from increased tissue protein breakdown (18). The finding that PDAC tumors have decreased utilization of circulating BCAAs contributes to this phenotype as well. In contrast, NSCLC tumors actively utilize BCAAs leading to plasma BCAA depletions, particularly since the liver does not regulate levels of these amino acids (23). Many patients with PDAC and NSCLC tumors develop cachexia with end-stage disease (39). Our findings suggest that differential use of amino acids by tumors and the resulting impact on whole body metabolism might play a role in the initiation and natural history of cachexia. In addition, as personalized medicine plays a larger role in the clinical management of cancer, it will be critical to understand how cell-of-origin and tissue environment interact with genetic events to influence metabolic dependencies of tumors and select the right treatment approaches for patients.

Supplementary Material

Refer to Web version on PubMed Central for supplementary material.

Acknowledgments

JRM acknowledges support from F30CA183474 and T32GM007753. ANL is a Robert Black Fellow of the Damon Runyon Cancer Research Foundation, DRG-2241-15. MGVH acknowledges support from P30CA1405141, R01CA168653, R01CA201276, the Burroughs Wellcome Fund, the Eisen and Chang Families, the Ludwig Center at MIT, SU2C, and the Lustgarten Foundation.

References

1. Garraway LA. Genomics-driven oncology: framework for an emerging paradigm. J Clin Oncol. 2013; 31:1806–1814. [PubMed: 23589557]
2. Vasan N, Boyer JL, Herbst RS. A RAS renaissance: emerging targeted therapies for KRAS-mutated non-small cell lung cancer. Clinical cancer research : an official journal of the American Association for Cancer Research. 2014; 20:3921–3930. [PubMed: 24893629]
3. Muller PA, Vousden KH. Mutant p53 in cancer: new functions and therapeutic opportunities. Cancer Cell. 2014; 25:304–317. [PubMed: 24651012]
4. Boroughs LK, DeBerardinis RJ. Metabolic pathways promoting cancer cell survival and growth. Nat Cell Biol. 2015; 17:351–359. [PubMed: 25774832]
5. White E. Exploiting the bad eating habits of Ras-driven cancers. Genes & Development. 2013; 27:2065–2071. [PubMed: 24115766]
6. Kruiswijk F, Labuschagne CF, Vousden KH. p53 in survival, death and metabolic health: a lifeguard with a licence to kill. Nat Rev Mol Cell Biol. 2015; 16:393–405. [PubMed: 26122615]
7. Biankin AV, et al. Pancreatic cancer genomes reveal aberrations in axon guidance pathway genes. Nature. 2012
8. N. Cancer Genome Atlas Research. Comprehensive molecular profiling of lung adenocarcinoma. Nature. 2014; 511:543–550. [PubMed: 25079552]
9. Vaupel P, Kallinowski F, Okunieff P. Blood Flow, Oxygen and Nutrient Supply, and Metabolic Microenvironment of Human Tumors: A Review. Cancer research. 1989
10. Hirayama A, et al. Quantitative metabolome profiling of colon and stomach cancer microenvironment by capillary electrophoresis time-of-flight mass spectrometry. Cancer research. 2009; 69:4918–4925. [PubMed: 19458066]
11. Mayers JR, Vander Heiden MG. Famine versus feast: understanding the metabolism of tumors in vivo. Trends Biochem Sci. 2015; 40:130–140. [PubMed: 25639751]
12. Commisso C, et al. Macropinocytosis of protein is an amino acid supply route in Ras-transformed cells. Nature. 2013; 497:633–637. [PubMed: 23665962]

13. Kamphorst JJ, et al. Hypoxic and Ras-transformed cells support growth by scavenging unsaturated fatty acids from lysophospholipids. Proceedings of the National Academy of Sciences of the United States of America. 2013; 110:8882–8887. [PubMed: 23671091]
14. Palm W, et al. The Utilization of Extracellular Proteins as Nutrients Is Suppressed by mTORC1. Cell. 2015
15. Davidson SM, et al. Environment Impacts the Metabolic Dependencies of Ras-Driven Non-Small Cell Lung Cancer. Cell Metab. 2016
16. Hu J, et al. Heterogeneity of tumor-induced gene expression changes in the human metabolic network. Nature biotechnology. 2013; 31:522–529.
17. Yuneva MO, et al. The Metabolic Profile of Tumors Depends on Both the Responsible Genetic Lesion and Tissue Type. Cell Metabolism. 2012; 15:157–170. [PubMed: 22326218]
18. Mayers JR, et al. Elevation of circulating branched-chain amino acids is an early event in human pancreatic adenocarcinoma development. Nature Medicine. 2014
19. Bardeesy N, et al. Both p16(Ink4a) and the p19(Arf)-p53 pathway constrain progression of pancreatic adenocarcinoma in the mouse. Proceedings of the National Academy of Sciences. 2006; 103:5947–5952.
20. DuPage M, Dooley AL, Jacks T. Conditional mouse lung cancer models using adenoviral or lentiviral delivery of Cre recombinase. Nature Protocols. 2009; 4:1064–1072. [PubMed: 19561589]
21. Harper A, Miller R, Block K. Branched-chain amino acid metabolism. Annual Review of Nutrition. 1984; 4:409–454.
22. Green CR, et al. Branched-chain amino acid catabolism fuels adipocyte differentiation and lipogenesis. Nat Chem Biol. 2016; 12:15–21. [PubMed: 26571352]
23. Brosnan JT. Interorgan amino acid transport and its regulation. The Journal of nutrition. 2003; 133:2068S–2072S. [PubMed: 12771367]
24. Birsoy K, et al. An Essential Role of the Mitochondrial Electron Transport Chain in Cell Proliferation Is to Enable Aspartate Synthesis. Cell. 2015; 162:540–551. [PubMed: 26232224]
25. Sullivan LB, et al. Supporting Aspartate Biosynthesis Is an Essential Function of Respiration in Proliferating Cells. Cell. 2015; 162:552–563. [PubMed: 26232225]
26. Hingorani SR, et al. Trp53R172H and KrasG12D cooperate to promote chromosomal instability and widely metastatic pancreatic ductal adenocarcinoma in mice. Cancer cell. 2005; 7:469–483. [PubMed: 15894267]
27. Friess H, et al. Diagnosis of pancreatic cancer by 2[18F]-fluoro-2-deoxy-D-glucose positron emission tomography. Gut. 1995; 36:771–777. [PubMed: 7797130]
28. Kubota K, et al. Differential diagnosis of lung tumor with positron emission tomography: a prospective study. J Nucl Med. 1990; 31:1927–1932. [PubMed: 2266388]
29. Nolop KB, et al. Glucose utilization in vivo by human pulmonary neoplasms. Cancer. 1987; 60:2682–2689. [PubMed: 3499969]
30. Barrett T, et al. NCBI GEO: archive for functional genomics data sets--10 years on. Nucleic acids research. 2011; 39:D1005–1010. [PubMed: 21097893]
31. Kamphorst JJ, et al. Human pancreatic cancer tumors are nutrient poor and tumor cells actively scavenge extracellular protein. Cancer Res. 2015; 75:544–553. [PubMed: 25644265]
32. Deberardinis RJ, et al. Beyond aerobic glycolysis: transformed cells can engage in glutamine metabolism that exceeds the requirement for protein and nucleotide synthesis. Proceedings of the National Academy of Sciences of the United States of America. 2007; 104:19345–19350. [PubMed: 18032601]
33. Marin-Valencia I, et al. Analysis of tumor metabolism reveals mitochondrial glucose oxidation in genetically diverse human glioblastomas in the mouse brain in vivo. Cell Metabolism. 2012; 15:827–837. [PubMed: 22682223]
34. Sellers K, et al. Pyruvate carboxylase is critical for non–small-cell lung cancer proliferation. The Journal of clinical investigation. 2015
35. Maher EA, et al. Metabolism of [U-13 C]glucose in human brain tumors in vivo. NMR in biomedicine. 2012; 25:1234–1244. [PubMed: 22419606]

36. Tardito S, et al. Glutamine synthetase activity fuels nucleotide biosynthesis and supports growth of glutamine-restricted glioblastoma. Nat Cell Biol. 2015; 17:1556–1568. [PubMed: 26595383]
37. Hensley CT, et al. Metabolic Heterogeneity in Human Lung Tumors. Cell. 2016; 164:681–694. [PubMed: 26853473]
38. Tönjes M, et al. BCAT1 promotes cell proliferation through amino acid catabolism in gliomas carrying wild-type IDH1. Nature Medicine. 2013; 19:901–908.
39. Dewys WD, et al. Prognostic effect of weight loss prior to chemotherapy in cancer patients. Eastern Cooperative Oncology Group. The American journal of medicine. 1980; 69:491–497. [PubMed: 7424938]
40. Clasquin, MF., Melamud, E., Rabinowitz, JD. LC-MS Data Processing with MAVEN: A Metabolomic Analysis and Visualization Engine. John Wiley & Sons, Inc; Hoboken, NJ, USA: 2002.
41. Antoniewicz MR, et al. Metabolic flux analysis in a nonstationary system: fed-batch fermentation of a high yielding strain of E. coli producing 1,3-propanediol. Metabolic engineering. 2007; 9:277–292. [PubMed: 17400499]
42. Fernandez CA, Des Rosiers C, Previs SF, David F, Brunengraber H. Correction of 13C mass isotopomer distributions for natural stable isotope abundance. Journal of mass spectrometry : JMS. 1996; 31:255–262. [PubMed: 8799277]
43. Yuan J, Bennett BD, Rabinowitz JD. Kinetic flux profiling for quantitation of cellular metabolic fluxes. Nature Protocols. 2008; 3:1328–1340. [PubMed: 18714301]
44. Vandesompele J, et al. Accurate normalization of real-time quantitative RT-PCR data by geometric averaging of multiple internal control genes. Genome Biol. 2002; 3:RESEARCH0034. [PubMed: 12184808]
45. Wu Z, Irizarry RA. Preprocessing of oligonucleotide array data. Nat Biotechnol. 2004; 22:656–658. author reply 658.
46. Smyth GK. Linear models and empirical bayes methods for assessing differential expression in microarray experiments. Statistical applications in genetics and molecular biology. 2004; 3 Article3.
47. Benjamini Y, Hochberg Y. Controlling the false discovery rate—a practical and powerful approach to multiple testing. J Roy Stat Soc B Met. 1995; 57:289–300.
48. Kanehisa M, Goto S, Furumichi M, Tanabe M, Hirakawa M. KEGG for representation and analysis of molecular networks involving diseases and drugs. Nucleic acids research. 2010; 38:D355–360. [PubMed: 19880382]
49. Commisso C, Flinn RJ, Bar-Sagi D. Determining the macropinocytic index of cells through a quantitative image-based assay. Nat Protoc. 2014; 9:182–192. [PubMed: 24385148]

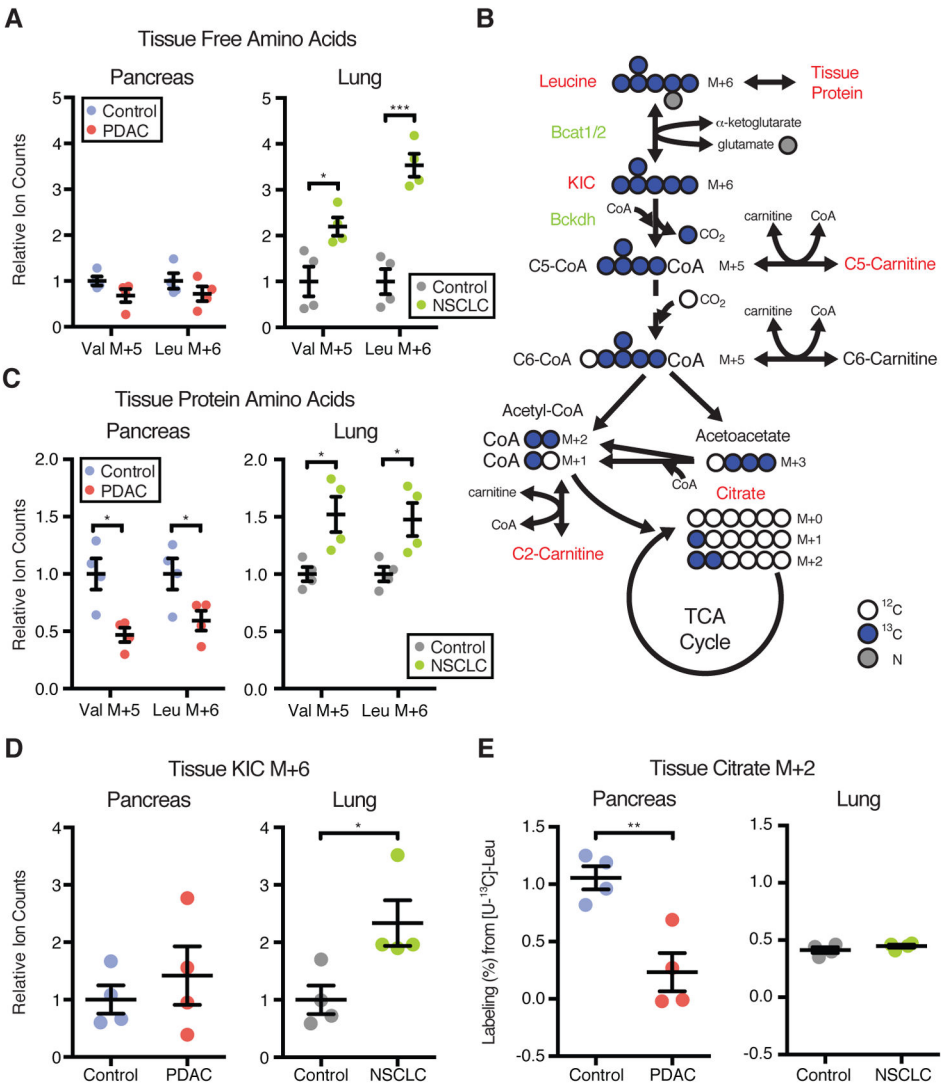

Fig. 1. Mice with NSCLC display increased BCAA uptake and metabolism

(**A** and **C–E**) Mice were fed ^{13}C-BCAA containing diet for seven days. (**A**) Relative ion counts by LC-MS analysis of fully-labeled, free BCAAs in tumors from PDAC and NSCLC mice and normal tissues from their respective control mice. Data are presented as mean ± SEM. $N = 4$ control and $N = 4$ PDAC; $N = 4$ control and $N = 4$ NSCLC. (**B**) Diagram of the leucine catabolic pathway. Red labels indicate metabolites measured by mass spectrometry. Blue circles indicate ^{13}C-labeled carbons. KIC = α-ketoisocaproate. (**C**) Relative ion counts by GC-MS analysis of fully-labeled BCAAs from protein acid hydrolysates of tumors from PDAC and NSCLC mice and normal tissues from their respective control mice. Data are presented as mean ± SEM. $N = 4$ control and $N = 4$ PDAC; $N = 4$ control and $N = 4$ NSCLC. (**D**) Relative ion counts by LC-MS analysis of fully-labeled KIC in tumors from PDAC and NSCLC mice and normal tissues from their respective control mice. Data are presented as mean ± SEM. $N = 4$ control and $N = 4$ PDAC; $N = 4$ control and $N = 4$ NSCLC. (**E**) Citrate M+2 labeling (%) from [U-^{13}C]-leucine by GC-MS analysis in tumors from PDAC and NSCLC mice and normal tissues from their respective control mice. Data

are presented as mean ± SEM. $N = 4$ control and $N = 4$ PDAC; $N = 4$ control and $N = 4$ NSCLC. Two-tailed *t* test was used for all comparisons between two groups. * $P<0.05$, ** $P<0.01$, *** $P<0.001$

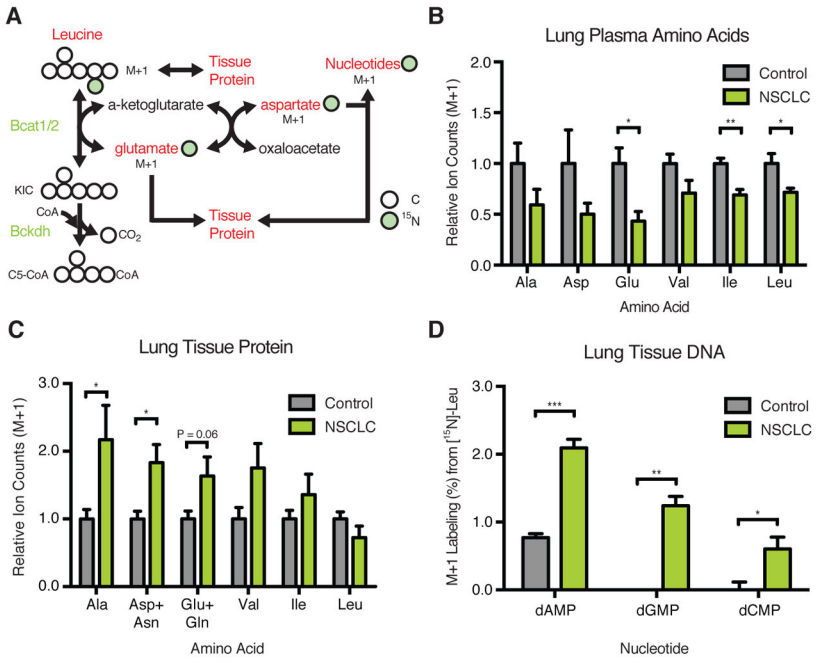

Fig. 2. BCAA-Derived Nitrogen Supports Non-Essential Amino Acid and DNA Synthesis in NSCLC tumors

(**A**) Diagram of leucine transamination by Branched-chain amino acid transferase (Bcat) and nitrogen (green circles) fate after transamination. (**B–D**) NSCLC mice were fed ^{15}N-leucine containing diet for six days. (**B**) Relative ion counts by GC-MS analysis of M+1 labeled amino acids in plasma of control and NSCLC mice. Data are presented as mean ± SEM. N = 5 control and N = 6 NSCLC. (**C**) Relative ion counts by GC-MS analysis of M+1 labeled amino acids from protein acid hydrolysates of control mouse lung tissue and NSCLC mouse tumors. Data are presented as mean ± SEM. N = 6 control and N = 6 NSCLC. (**D**) M+1 labeling (%) from ^{15}N-leucine of deoxynucleic acids from nucleic acid digest of control mouse lung tissue and NSCLC mouse tumors. Data are presented as mean ± SEM. N = 6 control and N = 6 NSCLC. Two-tailed t test was used for all comparisons between two groups. * P<0.05, ** P<0.01, *** P<0.001

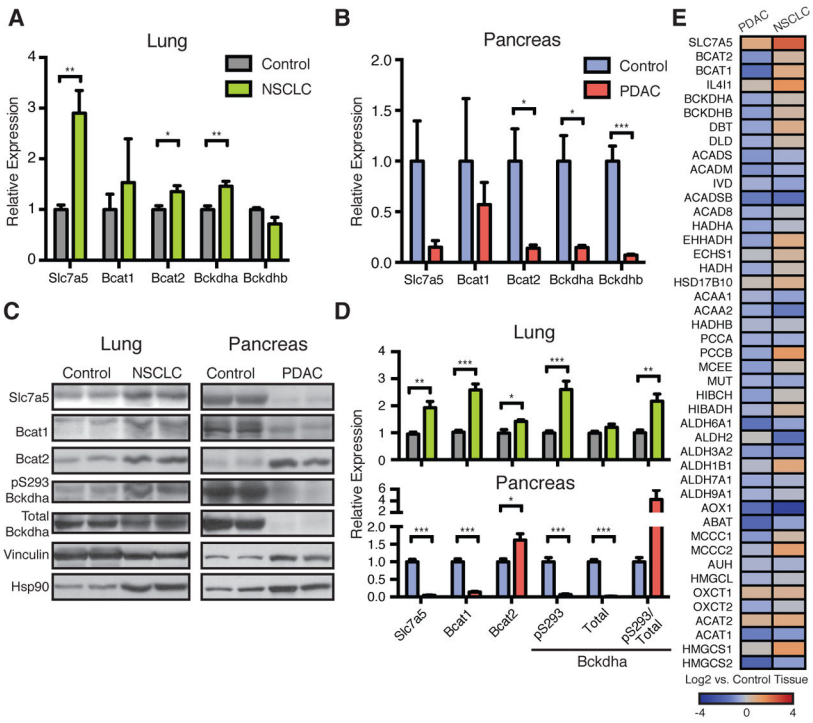

Fig. 3. Gene expression in both mouse and human tumors reflects tumor tissue-specific BCAA metabolism

(**A**) Relative Expression of BCAA metabolic pathway genes in normal lung and NSCLC tumors from KP mice. Data are presented as mean ± SEM. $N = 6$ control and $N = 6$ NSCLC. (**B**) Relative expression of BCAA metabolic pathway genes in normal pancreas and PDAC tumors from KP mice. Data are presented as mean ± SEM. $N = 7$ control and $N = 5$ PDAC. (**C**) Immunoblots of proteins involved in BCAA metabolism in representative normal lung and NSCLC tumors (left) and representative normal pancreas and PDAC tumors (right) from KP mice. (**D**) Quantification of (C). Data are presented as mean ± SEM. $N = 6$ control and $N = 6$ NSCLC; $N = 4$ control and $N = 4$ PDAC. (**E**) Comparison of BCAA metabolic pathway gene expression in human NSCLC and PDAC tumors relative to their adjacent paired normal tissues. Overall expression of BCAA metabolism genes is significantly decreased in PDAC ($P<0.0001$). Two-tailed t test was used for all comparisons between two groups unless otherwise stated. * $P<0.05$, ** $P<0.01$, *** $P<0.001$

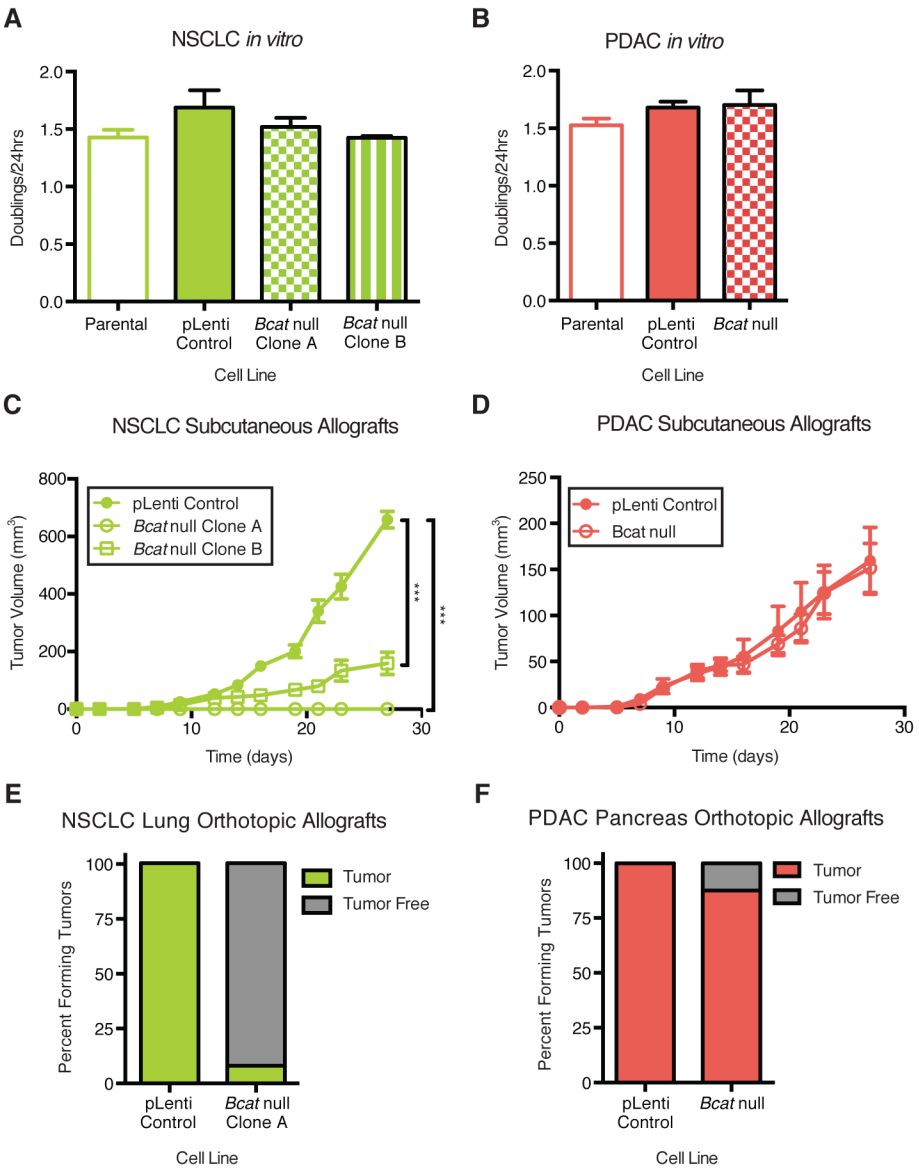

Fig. 4. Branched-chain amino acid transaminase (Bcat) activity is required for NSCLC tumor growth

(**A**) Doubling time of parental, control CRISPR-Cas9 vector infected (pLenti), and NSCLC *Bcat* null cell lines *in vitro*. Data are presented as mean ± SEM. $N = 3$ per group. Representative experiment from ≥ 2 repeats. (**B**) Doubling time of parental, control CRISPR-Cas9 vector infected and PDAC *Bcat* null cell lines *in vitro*. Data are presented as mean ± SEM. $N = 3$ per group. Representative experiment from ≥ 2 repeats. (**C**) Estimated tumor volume (mm^3) of subcutaneous allograft of control infected and *Bcat* null syngenic NSCLC cell lines into C57BL/6J mice. Data are presented as mean ± SEM. $N = 6$ per group. Two-way repeated measures *ANOVA* used for comparison between groups. (**D**) Estimated tumor volume (mm^3) of subcutaneous allograft of control infected and *Bcat* null syngenic PDAC cell lines into C57BL/6J mice. Data are presented as mean ± SEM. $N = 5$ pLenti control and $N = 6$ *Bcat* null. Two-way repeated measures *ANOVA* used for comparison

between groups. (**E**) Lung orthotopic allograft of control infected and *Bcat* null syngenic NSCLC cell lines into C57BL/6J mice. $N = 23$ vector control and $N = 13$ *Bcat* null Clone A. (**F**) Pancreatic orthotopic allograft of control infected and *Bcat* null syngenic PDAC cell lines into C57BL/6J mice. $N = 8$ per group. * $P<0.05$, ** $P<0.01$, *** $P<0.001$.